PGK1, a promising biomarker and therapeutic target for patients with acute myeloid leukemia who are susceptible to disease relapse

Junyan Gao
Affiliated Hospital of Yangzhou University https://orcid.org/0000-0001-6678-6147
Xinran Chu
Children's Hospital of Soochow University
Shan He
Children's Hospital of Soochow University
Li Gao
Children's Hospital of Soochow University
Hui Hou
Inner Mongolia People's Hospital
Fang Fang
Children's Hospital of Soochow University
Jian Pan
Children's Hospital of Soochow University
Shaoyan Hu (hushaoyan@suda.edu.cn)
https://orcid.org/0000-0002-3386-6957

Primary research

Keywords: phosphoglycerate kinase 1, acute myeloid leukemia, relapse, survival biomarker, therapeutic target

Posted Date: July 14th, 2020

DOI: https://doi.org/10.21203/rs.3.rs-41160/v1

Abstract

Background: Glycolysis, a multi-step enzymatic reaction, is considered to be the root of cancer development and progression. The aim of this study is to figure out the glycolytic enzyme, phosphoglycerate kinase 1 (PGK1) whether participate in the progression of acute myeloid leukemia (AML) and its possible mechanisms.

Methods: Four datasets (GSE106096, GSE75086, GSE107968 and GSE106748) containing 30 leukemic blast cell samples of AML at diagnosis, 17 leukemic blast cell samples of AML relapse and 3 bone marrow CD34+ cell samples of healthy donors were downloaded from Gene Expression Omnibus (GEO) database and PGK1 was screened out as a potential survival biomarker in AML. Then we did a series of clinical sample verifications and gene set enrichment analysis (GSEA) focusing on PGK1. We further knocked down expression of PGK1 in myelogenous leukemia cell lines and explored its potential effects.

Results: PGK1 expression was up-regulated among AML at diagnosis versus healthy control, AML relapse versus AML at diagnosis and AML relapse versus healthy control datasets. Through a serial of bioinformatic analyses (differentially expressed genes [DEGs] selection, function and pathway enrichments and protein-protein interaction [PPI] network establishment), PGK1 was identified as the most meaningful gene in AML progression. Furthermore, the generally high expression of PGK1 was confirmed in AML samples comparing with healthy controls in our single center and the high-expression PGK1 was associated with a comparatively low complete remission (CR) rate, a significantly high 5-year cumulative incidence of relapse (CIR), a poor 5-year event-free survival (EFS) rate, and a poor 5-year overall survival (OS) rate. The GSEA revealed that high-expression PGK1 in AML was associated with many pathways including cytosolic DNA sensing, pentose phosphate, base excision repair and DNA replication. *In vitro*, the transfected U937 and K562 cells with PGK1 knock-down showed decreased cell viability and increased apoptotic rate. PGK1 inhibition could greatly decrease the half maximal inhibitory concentrations (IC50) of cytarabine (Ara-C) and daunorubicin (DNR) in U937 and K562 cell lines.

Conclusions: High-expression PGK1 was associated with poor prognosis in AML. PGK1 may serve to predict the AML progression and provide a novel therapeutic target for AML.

Background

In spite of accepted standard treatments, about 40–60% of newly diagnosed acute myeloid leukemia (AML) patients and 30–50% of those after allogenetic hematopoietic stem cell transplantation (allo-HSCT) still face the risk of relapse which remains a tough challenge and indicates a poor prognosis (1, 2). Due to the intrinsic heterogeneity of AML and acquired drug resistance of tumor cells, current chemotherapy drugs and molecular targeted agents exhibit suboptimal effects (3–5). The basis of clonal evolution and disease relapse in AML is poorly understood and novel therapeutic targets with wide spectrum are urgently needed.

It is universally acknowledged that cancer cells can switch their metabolic pattern depending on the tumor microenvironment (TME) and preferentially use aerobic glycolysis rather than oxidative phosphorylation (that is the Warburg effect) since it is 10–100 times more rapid of energy generation (6, 7). The glycolytic enzymes enable death resistance of shed cancer cells and facilitate tumor recurrence and disease relapse (8, 9). Phosphoglycerate kinase 1 (PGK1), as a glycolytic enzyme and a newly identified protein kinase, coordinates glycolysis and mitochondrial metabolism (10). PGK1 is one of the only two glycolytic enzymes that can generate adenosine triphosphate (ATP) in the glycolytic pathway (11). In addition, it is demonstrated that PGK1 could be translocated into the mitochondria and act as a protein kinase (10, 12). Mitochondrial PGK1 phosphorylates pyruvate dehydrogenase kinase 1 (PDHK1) which could lead to the suppression of pyruvate utilization, reduction of oxidative products, accumulation of lactate and proliferation of tumor cells. Moreover, PGK1 could participate in inflammation, immune response and autophagy with non-metabolic functions and also moonlights as a transcription factor to promote DNA replication (13–17). Series of studies revealed that PGK1 is overexpressed in a variety of tumors (such as cancers of stomach, colon, breast and liver) (18–22). The elevated PGK1 expression significantly increased the malignancy degree and indicated a poor prognosis (18–20, 23). However, the influence of PGK1 on AML is rarely evaluated.

In the present study, we firstly performed a bioinformatical analysis and screened out PGK1 as a potential survival biomarker in AML. Then we did a series of clinical sample verifications and gene set enrichment analysis (GSEA) focusing on PGK1. We further knocked down expression of PGK1 in myelogenous leukemia cell lines and explored its potential effects. We found the high-expression PGK1 was associated with poor prognosis in AML and knocking down PGK1 expression could suppress the myelogenous leukemia cells' proliferation.

Methods

Microarray data

Four datasets (GSE106096, GSE75086, GSE107968 and GSE106748) containing 30 leukemic blast cell samples of AML at diagnosis, 17 leukemic blast cell samples of AML relapse and 3 bone marrow CD34+ cell samples of healthy donors were downloaded from Gene Expression Omnibus (GEO) database (http://www.ncbi.nlm.nih.gov/geo) (Illumina GPL10558 platform, Illumina HumanHT-12 V4.0 expression beadchip; Affymetrix GPL16686 platform, Affymetrix Human Gene 2.0 ST Array; Affymetrix GPL570 platform, Affymetrix Human Genome U133 Plus 2.0 Array). Then, the four datasets were normalized by log2 conversion and merged as three expression matrices (AML at diagnosis versus healthy control, AML relapse versus AML at diagnosis and AML relapse versus healthy control). The probes were converted into the corresponding gene symbol based on the annotation information of the platforms. In addition, the probe sets without corresponding gene symbols were removed and genes with more than one probe set were averaged respectively by using R software (version 3.6.2).

Identification of differentially expressed genes (DEGs)

The study batch effect was adjusted by using Cochran's Q test for the three expression matrices and the meta-analysis (Combining Effect Sizes method) was adopted to determine the DEGs between groups (a p-value<0.05 was considered statistically significant). The DEGs screened out by meta-analysis through Lima package of R software (version 3.6.2) were further selected by a criterion of |logFC (fold-change)| >1 and adj. P-value <0.01. Then, the Venn diagram was adopted to identify intersection of DEGs from aforementioned three matrices.

KEGG and GO enrichment analyses of DEGs

The Database for Annotation, Visualization and Integrated Discovery (DAVID; http://david.ncifcrf.gov, version 6.8) was employed as a tool to analyze the biological information of DEGs mentioned above (24). Kyoto Encyclopedia of Genes and Genomes (KEGG) is a database resource for understanding high-level functions and biological systems from large-scale molecular datasets generated by high-throughput experimental technologies and Gene Ontology (GO) is a major bioinformatics tool to annotate genes and analyze biological process of these genes (25, 26). Both of KEGG and GO functions are integrated in DAVID. P<0.05 was considered statistically significant.

PPI network construction and module analysis

The Search Tool for the Retrieval of Interacting Genes (STRING; http://string-db.org, version 11.0) was used to predict and establish the protein-protein interaction (PPI) network of DEGs. By analysis module of STRING, a set of combined scores which represented the interaction strength of the proteins were calculated (low=0.15; medium=0.4; high=0.7; highest=0.9 for instance). An interaction with a combined score >0.4 was considered statistically significant while nodes without connections were ruled out. Then, the Cytoscape software (version 3.7.2) was employed for visualizing molecular interaction networks and the Molecular Complex Detection (MCODE) plug-in of Cytoscape was adopted for identifying the most significant modules in the PPI network based on topology. The criteria for selections was as follows: MCODE scores ≥10, degree cut-off=2, node score cut-off=0.2, Max depth=100 and k-score=2.

Hub genes selection and analysis

After the most significant modules were determined by MCODE, the plug-in cytoHubba of Cytoscape was used to rank the genes by EPC method and genes with degree ≥10 were determined as hub genes.

Patients and ethics statement

For clinical verification, a total of 50 AML patients and 10 healthy donors were enrolled in this study at Children's Hospital of Soochow University. These patients were newly diagnosed with AML as defined by the World Health Organization (WHO) criteria (27) from October 2013 to October 2015 and were followed up every month and the follow-up endpoint was April 31, 2020. Patients with promyelocytic leukemia, myelodysplastic syndrome-related AML, treatment-related AML and AML of Down syndrome were not included in this study. This study was approved by the hospital ethics committee of Children's Hospital of

Soochow University and written informed consents were obtained from the parents or guardians of all patients and donors.

Quantitative real-time polymerase chain reaction (qRT-PCR)

The bone marrow (BM) samples were collected prior to treatment and mononuclear cells (MNCs) were enriched through Ficoll gradient centrifugation immediately and stored at -80°C. Total RNA of MNCs samples were extracted using TRIzol reagent (Invitrogen) and reverse-transcribed into cDNA using the reverse transcription kit (Takara). The qRT-PCR was employed to measure the levels of mRNAs using the comparative Ct method. GAPDH was considered as the normalization control for mRNA. All primers for qRT-PCR were listed in Supplementary Table 1.

Evaluations and follow-ups

Patients were treated by stratified treatment according to the risk stratification criteria (28-31). Response was evaluated on day 26 of each induction chemotherapy course. Complete remission (CR) was defined as white blood cell (WBC) $\geq 1.0*10^9$/L, absolute neutrophil count (ANC) $\geq 0.5*10^9$/L, platelet count (PLT) $\geq 50*10^9$/L and BM blast cells <5%. The overall survival time (OS) was calculated from the date of diagnosis to the date of death or last follow-up. The events included death, relapse and secondary tumor. The event-free survival time (EFS) was defined as the survival time without those events since the date of diagnosis. Relapse was defined as the recurrence of blasts ≥5% in BM after CR status. The relapse-free survival time (RFS) was calculated from the date of diagnosis to the date of first relapse or last follow-up and the cumulative incidence of relapse (CIS) was calculated.

Gene set enrichment analysis (GSEA)

GSEA is a computational method that assesses whether a set of prior defined genes shows statistically significant and concordant differences between two biological states (32). To investigate the role of PGK1 in AML, GSEA was conducted to analyze the enrichment of datasets between high-expression PGK1 (defined as the mRNA level higher than the median level) and low-expression PGK1 (defined as the mRNA level lower than the median level) groups. False discovery rate (FDR) <25% and nominal $p<0.05$ were set as the cut-off criterion.

Cell lines and cell culture

The human acute myelogenous leukemia cell lines (HL-60, NB4, U937 and SHI-1 cell lines) and chronic myelogenous leukemia cell line (K562 cell line) were obtained from Jiangsu Institute of Hematology. All these myelogenous leukemia cell lines were cultured in Roswell Park Memorial Institute (RPMI) 1640 medium and supplemented with 10% fetal bovine serum (FBS) and 1% penicillin-streptomycin. The 293FT cell line derived from the primary embryonal human kidney which is suitable for generating lentiviral constructs was purchased (Invitrogen) and cultured in Dulbecco's modified eagle's medium

(DMEM) containing 10% FBS and 1% penicillin-streptomycin. All the cell lines were cultured in a 37℃ humidified incubator containing 5% CO_2.

Transfection of PGK1

Small hairpin RNA for knocking down expression of PGK1 (shPGK1) with a lentiviral vector was transfected into the myelogenous leukemia cells for at least 48h. A lentiviral vector without shPGK1 aliased as shNC was used as a negative control. Detailed schedule was shown in Supplementary Fig.1.

Cell viability evaluation

Transfected myelogenous leukemia cells were seeded in the 96-well plate at a concentration of $2*10^4$ cells/well and incubated at 37℃ for one to five days. 10ul of Cell Counting Kit-8 (CCK-8) was added to each well and incubated at 37℃ for 4h. The cell proliferation was measured by the microplate reader at the absorbance at 450nm of optimal density (OD_{450nm}).

Cell apoptosis assay

Cellular apoptosis was quantified by flow cytometry using Annexin V-FITC (BD Pharmingen) following the manufacturer's protocol.

Western blotting (WB)

Cells were harvested, washed and lysed in radioimmunoprecipitation assay buffer (RIPA) containing 1mM phenylmethylsulfonyl fluoride (PMSF) and protease inhibitor according to the manufacturer's protocol (Sigma). The protein concentration was measured with BCA Protein Assay Kit (Pierce). All samples were loaded and electrophoresed on 10-15% sodium salt polyacrylamide gel electrophoresis (SDS-PAGE) gels and transferred onto polyvinylidene fluoride (PVDF) membranes (Millipore). After being blocked with 10% BSA for 2 hours, the membranes were incubated with a specific primary antibody overnight at 4℃, washed with tris-buffered saline and Tween 20 (TBST) and then incubated with a secondary antibody for one hour. Primary antibodies used in this study were as follows: monoclonal anti-PGK1, GAPDH (Abcam), Bax, Bcl-2, Cleaved PRAP, Cleaved Caspase-3 and β-actin (Cell Signaling Technology). For secondary antibodies, horseradish peroxidase (HRP)-conjugated goat anti-mouse or goat anti-rabbit IgG (Cell Signaling Technology) was used. The Pierce Enhanced Chemiluminescence (Thermo Scientific) was applied for blots and the band density was analyzed by using Image Processing and Analysis in Java (Image J, verson 1.8.0) software.

Half maximal inhibitory concentration (IC50) calculation

The transfected myelogenous leukemia cells with shPGK1 or shNC were treated with chemotherapeutic agents (cytarabine [Ara-C] and daunorubicin [DNR]) for 24h and 48h. Afterwards, the cell viability was examined by CCK-8 assay. The drug concentration and corresponding OD_{450nm} values were imported and the IC50 was calculated by SPSS software through a nonlinear regression analysis.

Statistic analysis

The descriptive statistics included the median and range for continuous variables as well as the number and percentage of categorical variables. The independent Student's t-test was utilized to compare normal distributional variables while the Mann-Whitney U test was used to assess skewed distributional variables. The categorical variables were analyzed using Chi square or Fisher's Exact Test, as appropriate. The survival functions (CIR, EFS and OS) were described by Kaplan-Meier methods and the log-rank test was used to compare the survival curves. Furthermore, the risk factors of AML were evaluated through Cox regression analysis. SPSS 26.0 software was employed for data processing. Prism 8.0 software was served for results visualization. $P<0.05$ was considered to be statistically significant.

Results

DEGs identification

The four gene expression datasets were standardized by log2 conversion and merged as three expression matrices (Supplementary Fig.2). The DEGs between groups were shown as heatmaps and volcano plots (Fig.1a and Fig.1b). According to the intersection obtained from the Venn diagram, eventually, 41 common DGEs were identified (Fig.1c).

KEGG and GO enrichment analyses of DEGs

Through DAVID website, function and pathway enrichments of DEGs were analyzed. The KEGG pathway results revealed that the DEGs were mainly enriched in glycolysis/gluconeogenesis, carbon metabolism, biosynthesis of amino acids and pentose phosphate pathway (Fig.2a). The biological processes (BP) of DEGs by GO analysis were mainly enriched in immune response, collagen-activated signaling pathway, leukocyte degranulation and myeloid cell activation involved in immune response (Fig.2b). The cellular components (CC) were mainly enriched in tertiary granule, specific granule, secretory granule and cytoplasmic vesicle lumen (Fig.2c). The molecular functions (MF) were mainly enriched in collagen receptor activity, translation factor activity, RNA binding, IgG binding and immunoglobulin binding (Fig.2d).

PPI network construction and hub genes identification

The PPI network of the common DEGs was constructed (Fig.3a) containing 40 nodes and 558 edges except one DEG, which was excluded due to no connection with others. The most significant clusters were obtained by using plug-in MCODE of Cytoscape, which contains 32 nodes and 475 edges. These 32 nodes were considered as the hub genes and ranked by the plug-in cytoHubba of Cytoscape (Fig.3b). The depth of color represented the different scores calculated by cytoHubba and the darker of the node, the higher the score was. The names, abbreviations, functions and EPC scores for these 32 hub genes are shown in Table 1.

Expressions of key genes in AML samples

The top eight hub genes (PGK1, PFKL, GPI, ALDOC, TPI1, PFKP, HK2 and ALDOA) were further verified by qRT-PCR through AML patients' and healthy donors' samples in our center. PGK1 was much higher expressed in AML samples with a p-value<0.001 (Fig.4a). PFKP also showed significant difference between groups with a p-value=0.018 (Fig.4a). While PFKL, GPI, ALDOC, TPI1, HK2 and ALDOA showed no significant difference between groups (Fig.4a). Then, the AML patients were divided into two groups (low-expression group and high-expression group) by the median mRNA level of PGK1 and PFKP, respectively. There was no significant difference in gender, age at diagnosis, blood cell counts at diagnosis, main types of fusion gene and gene mutation, cytogenetics and French-American-British (FAB) classification between high-expression PGK1 and low-expression PGK1 groups (Table 2). With respect to risk stratification, there were more patients with high risk (n=10) and fewer patients with low risk (n=7) in high-expression PGK1 group comparing patients in low-expression PGK1 group (P=0.019) (Table 2). The high-expression PGK1 was related to a comparatively low CR rate of induction chemotherapy (56.0% versus 88.0%, P=0.027 of induction I and 72.0% versus 96.0%, P=0.054 of induction II, Table 2), a significantly poor 5-year EFS (31.1±9.4% versus 88.0±6.5%，P<0.001), a significantly poor 5-year OS (56.0±9.9% versus 88.0±6.5%, P=0.007) and a significantly high 5-year CIR (47.0±13.2% versus 4.3±4.3%, P=0.001) (Fig.4b). While groups between the high-expression and low-expression PFKP showed no statistical significance (Fig.4b). In addition, high-expression PGK1 was determined as a risk factor of RFS, EFS and OS through the Cox regression analyses (Supplementary Table 2).

GSEA of PGK1

To better understand the function of PGK1 and signaling pathways activated in AML, we applied GSEA comparing the datasets of low-expression and high-expression PGK1. The results showed the gene sets associated with cytosolic DNA sensing pathway, pentose phosphate pathway, base excision repair and DNA replication pathway were differentially enriched with the phenotype of high-expression PGK1 (Fig.5a) and the gene sets associated with apoptosis, biosynthesis of unsaturated fatty acids, glycosaminoglycan biosynthesis chondroitin sulfate and other glycan degradation were differentially enriched with the phenotype of low-expression PGK1 (Fig.5b).

Transfection of shPGK1

The mRNA and protein level of PGK1 on the five selected myelogenous leukemia cell lines were detected by qRT-PCR and WB respectively (Supplementary Fig.3). Then, the U937 and K562 cell lines with relatively high expression of PGK1 were chosen for the following transfection experiments. The sequence two (PGK1-sh2) was used for further functional verifications due to its highest stable transfection efficiency for at least five to nine days (Fig.6a).

PGK1's effects on cell proliferation and apoptosis

From the CCK-8 assay for more than three days after transfection, decelerated proliferation of shPGK1 treated cells were observed and these demonstrated the effects of PGK1 on the growth and viability of U937 and K562 cells (Fig.6b). To further investigate the cell viability with PGK1 knocked-down, the

apoptotic rate was assayed by flow cytometer and apoptosis-indicated proteins were measured by WB. The percentage of apoptotic cells in both two cell lines treated with shPGK1 were significantly higher than that of shNC group (12.50±0.54% versus 4.90±0.66%, P<0.001 and 10.62±0.97% versus 4.89±0.79%, P=0.001 for U937 and K562 cells respectively) (Fig.6c). Correspondingly, a clear decrease of Bcl-2 and an increase of Bax were obtained after shPGK1 transfection. The indicators of apoptosis activation, the PARP cleavage and Caspase-3 cleavage were significantly increased (Fig.6d).

IC50 calculation

The U937 and K562 cells were treated with different concentrations of chemotherapeutic agents with a combination of shPGK1 or shNC and examined by CCK-8 assay (Fig.6e). A maximal cytogenetic effect on tumor cells was found after the combined therapy of chemotherapeutic agents and shPGK1 (Fig.6e and Table 3). Surprisingly, the IC50 of DNR on shPGK1 transfected U937 cells showed an approximate 1/7 value of shNC transfected one (1.865μmol/L versus 13.360μmol/L) (Table 3).

Discussion

AML is characterized with molecular heterogeneity and many patients remain refractory and relapse. So far, little is known about how the clones evolve during disease relapse and progression. It seems that RNA based changes may play a crucial role in the development and progression of AML and also, AML relapse may share a common biological process (33–35).

We identified a common biological pattern associated with disease progression covering various AML molecular subtypes through a database mining and bioinformatical analyses in the first part of the study. A cluster of co-overexpression genes linked to relapse and progression risk in distinct patient subgroups were identified. Accordingly, quite a few of the 32 DEGs screened out as hub genes were sorted to be glycolytic enzymes (such as PGK1, PFKL, ALDOC, ENO1 and so on presented in Table 1). In addition, those hub genes were mainly involved in glycolysis/gluconeogenesis, carbon metabolism, biosynthesis of amino acids and pentose phosphate pathway. It could be inferred that metabolic changes especially glycolysis might be associated with disease recurrence and progression in AML. This result was consistent with previous studies, of which, the enhanced glycolysis achieved by multiple tumors was proposed (23, 36–38).

In the present study, PGK1 showed the highest EPC score of 13.198 and was confirmed to be the most significantly expressed either in datasets or in clinical sample verifications. High-expression PGK1 is related to a high incidence of relapse and a poor prognosis suggesting that PGK1 may play an important role in the progression of AML. PGK1 is a glycolytic enzyme which catalyze one of the two ATP producing reactions and also has been identified as a moonlighting protein to perform multi-functions involved in DNA replication, immune response, inflammation, autophagy and so on (10, 12–16, 39, 40). Consistently, our GSEA results revealed that high-expression PGK1 in AML were associated with many pathways including cytosolic DNA sensing, pentose phosphate, base excision repair and DNA replication. In addition, the shPGK1 lentivirus vector was constructed and the PGK1 mRNA and protein expression level

could be efficiently knocked down in myelogenous leukemia cell lines. The inhibition of cell proliferation and induction of cell apoptosis were observed with shPGK1 compared with negative controls. Basesd on the results above, it could be inferred that PGK1 might influence the biological progression of AML through multiple functions and pathways.

Moreover, the IC50 was greatly decreased by combination of chemotherapeutic agents and shPGK1 which indicated the role of PGK1 in chemotherapy sensitivity. PGK1 might influence the inherent and acquired treatment resistance of acute myeloid leukemic cells. The specific PGK1-invovled mechanism for chemotherapy sensitivity in AML needs further explored.

Several limitations about our study should be considered. Firstly, due to the heterogeneity of AML populations, the DEGs identified from the four datasets which were adjusted by study batch effect may not be accurately suitable for individual leukemic blast sample. Secondly, owing to the small size of clinical samples (a total of 50 AML patients and 10 healthy donors), further expanding the sample size to obtain more sturdy results is necessary. Thirdly, we've just explored the initial effects of PGK1 *in vitro* and the more specific and in-depth researches are required in the future.

In summary, our study has identified the common biological pathways involved in the progression of AML. Several key genes were screened out and further verified by clinical samples. PGK1 is one of the most significant gene that highly up-regulated in AML and PGK1 may have the potential for predicting the risk of relapse and poor prognosis of AML patients. Inhibition of PGK1 may be utilized in synergy with existing treatments. Further studies focusing on precise mechanism and subgroups benefit most from PGK1-targeted treatment need to be explored.

Conclusions

Our study established a common gene signature involved in AML progression and demonstrated that PGK1 might play an important role in AML progression which could be a novel therapeutic target for AML.

Abbreviations

AML: acute myeloid leukemia; ANC: absolute neutrophil count; Ara-C: cytarabine; ATP: adenosine triphosphate; BM: bone marrow; BP: biological process; CC: cellular component; CCK-8: Cell Counting Kit-8; CIR: cumulative incidence of relapse; CR: complete remission; DAVID: Database for Annotation, Visualization and Integrated Discovery; DEG: differentially expressed gene; DMEM: Dulbecco's modified eagle's medium; DNR: daunorubicin; FBS: fetal bovine serum; FC: fold-change; FDR: false discovery rate; EFS: event-free survival; GEO: Gene Expression Omnibus; GO: Gene Ontology; GSEA: gene set enrichment analysis; HRP: horseradish peroxidase; HSCT: hematopoietic stem cell transplantation; IC50: half maximal inhibitory concentration; KEGG: Kyoto Encyclopedia of Genes and Genomes; MCODE: Molecular Complex Detection; MF: molecular function; MNC: mononuclear cell; OD: optimal density; OS: overall

survival; PDHK1: pyruvate dehydrogenase kinase 1; PGK1: phosphoglycerate kinase 1; PLT: platelet count; PMSF: phenylmethylsulfonyl fluoride; PPI: protein-protein interaction; PVDF: polyvinylidene fluoride; RFS: relapse-free survival; RIPA: radioimmunoprecipitation assay buffer; RPMI: Roswell Park Memorial Institute; RT-PCR: real-time polymerase chain reaction; SDS-PAGE: sodium salt polyacrylamide gel electrophoresis; STRING: Search Tool for the Retrieval of Interacting Genes; TBST: tris-buffered saline and Tween 20; TME: tumor microenvironment; WB: western blotting; WBC: white blood cell; WHO: World Health Organization.

Declarations

Ethics approval and consent to participate

This study was approved by the hospital ethics committee of Children's Hospital of Soochow University and written informed consents were obtained from the parents or guardians of all patients and donors.

Consent for publication

Not applicable.

Availability of data and materials

The part of original data for bioinformatical analysis can be found at GEO database (http://www.ncbi.nlm.nih.gov/geo) and the part of the clinical and the experimental data could be obtained from the authors if the editor or reviewer request.

Competing interests

The authors declare that they have no competing interests.

Funding

This work was supported by the Natural Science Foundation of China (NO. 81770193, 81700165 and 81970163), Jiangsu Province Projects (NO. CXTDA2017014, BE2017659 and BE2017658), Suzhou projects (NO. SS201809 and SZZX201504), and National Clinical Research Center for Hematological Disorders.

Authors' contributions

Shaoyan Hu contributed to conception, design, acquisition, analysis, and interpretation of data. Junyan Gao contributed to the acquisition of data and manuscript preparation. Xinran Chu and Shan He contributed to the conception, analysis, and interpretation of data. Li Gao, Hui Hou and Fang Fang contributed to the interpretation of data. Shaoyan Hu and Jian Pan conducted the study, and revised the manuscript critically. All the authors participated in the discussion and editing of the manuscript. All authors read and approved the fnal manuscript.

Acknowledgment

Not applicable.

References

1. Tsirigotis P, Byrne M, Schmid C, Baron F, Ciceri F, Esteve J, et al. Relapse of AML after hematopoietic stem cell transplantation: methods of monitoring and preventive strategies. A review from the ALWP of the EBMT. Bone Marrow Transplant. 2016;51(11):1431–8.
2. Wayne AS, Giralt S, Kroger N, Bishop MR. Proceedings from the National Cancer Institute's Second International Workshop on the Biology, Prevention, and Treatment of Relapse after Hematopoietic Stem Cell Transplantation: introduction. Biol Blood Marrow Transplant. 2013;19(11):1534-6.
3. Shlush LI, Mitchell A. AML evolution from preleukemia to leukemia and relapse. Best Pract Res Clin Haematol. 2015;28(2–3):81–9.
4. Jonas BA. On the origin of relapse in AML. Science Translational Medicine. 2017;9(398).
5. Vosberg S, Greif PA. Clonal evolution of acute myeloid leukemia from diagnosis to relapse. Genes Chromosomes Cancer. 2019;58(12):839–49.
6. Warburg O, Wind F, Negelein E. The metabolism of tumor in the body. J Gen Physiol. 1926; 519–530.
7. Weber GF. Metabolism in cancer metastasis. Int J Cancer. 2016;138(9):2061–6.
8. Porporato PE, Dhup S, Dadhich RK, Copetti T, Sonveaux P. Anticancer targets in the glycolytic metabolism of tumors: a comprehensive review. Front Pharmacol. 2011;2:49.
9. Huang R, Zong X. Aberrant cancer metabolism in epithelial-mesenchymal transition and cancer metastasis: Mechanisms in cancer progression. Crit Rev Oncol Hematol. 2017;115:13–22.
10. Li X, Jiang Y, Meisenhelder J, Yang W, Hawke DH, Zheng Y, et al. Mitochondria-Translocated PGK1 Functions as a Protein Kinase to Coordinate Glycolysis and the TCA Cycle in Tumorigenesis. Mol Cell. 2016;61(5):705–19.
11. Yu L, Chen X, Sun X, Wang L, Chen S. The Glycolytic Switch in Tumors: How Many Players Are Involved? J Cancer. 2017;8(17):3430–40.
12. Lu Z, Hunter T. Metabolic Kinases Moonlighting as Protein Kinases. Trends Biochem Sci. 2018;43(4):301–10.
13. Seki SM, Gaultier A. Exploring Non-Metabolic Functions of Glycolytic Enzymes in Immunity. Front Immunol. 2017;8:1549.
14. Yu X, Li S. Non-metabolic functions of glycolytic enzymes in tumorigenesis. Oncogene. 2017;36(19):2629–36.
15. Qian X, Li X, Cai Q, Zhang C, Yu Q, Jiang Y, et al. Phosphoglycerate Kinase 1 Phosphorylates Beclin1 to Induce Autophagy. Mol Cell. 2017;65(5):917–31. e6.
16. Li X, Zheng Y, Lu Z. PGK1 is a new member of the protein kinome. Cell Cycle. 2016;15(14):1803–4.

17. Zieker D, Konigsrainer I, Tritschler I, Loffler M, et al. Phosphoglycerate kinase 1 a promoting enzyme for peritoneal dissemination in gastric cancer. Int J Cancer. 2010;126(6):1513–20.
18. Sun S, Liang X, Zhang X, Liu T, Shi Q, Song Y, et al. Phosphoglycerate kinase-1 is a predictor of poor survival and a novel prognostic biomarker of chemoresistance to paclitaxel treatment in breast cancer. Br J Cancer. 2015;112(8):1332–9.
19. Ahmad SS, Glatzle J, Bajaeifer K, Buhler S, Lehmann T, Konigsrainer I, et al. Phosphoglycerate kinase 1 as a promoter of metastasis in colon cancer. Int J Oncol. 2013;43(2):586–90.
20. Zieker D, Konigsrainer I, Traub F, Nieselt K, et al. PGK1 a potential marker for peritoneal dissemination in gastric cancer. Cell Physiol Biochem. 2008;21(5–6):429–36.
21. Hu H, Zhu W, Qin J, Chen M, Gong L, Li L, et al. Acetylation of PGK1 promotes liver cancer cell proliferation and tumorigenesis. Hepatology. 2017;65(2):515–28.
22. Schneider CC, Archid R, Fischer N, Buhler S, Venturelli S, Berger A, et al. Metabolic alteration–Overcoming therapy resistance in gastric cancer via PGK-1 inhibition in a combined therapy with standard chemotherapeutics. Int J Surg. 2015;22:92–8.
23. Ganapathy-Kanniappan S, Geschwind JF. Tumor glycolysis as a target for cancer therapy: progress and prospects. Mol Cancer. 2013;3:12:152.
24. Huang DW, Sherman BT, Tan Q, Collins JR, Alvord WG, Roayaei J, et al. The DAVID Gene Functional Classification Tool: a novel biological module-centric algorithm to functionally analyze large gene lists. Genome Biol. 2007;8(9):R183.
25. Kanehisa M, Furumichi M, Tanabe M, Sato Y, Morishima K. KEGG: new perspectives on genomes, pathways, diseases and drugs. Nucleic Acids Res. 2017;45(D1):D353-D61.
26. Gene Ontology C. Gene Ontology Consortium: going forward. Nucleic Acids Res. 2015;43(Database issue):D1049-56.
27. Arber DA, Orazi A, Hasserjian R, Thiele J, Borowitz MJ, Le Beau MM, et al. The 2016 revision to the World Health Organization classification of myeloid neoplasms and acute leukemia. Blood. 2016;127(20):2391–405.
28. Strickland SA, Shaver AC, Byrne M, Daber RD, Ferrell PB, Head DR, et al. Genotypic and clinical heterogeneity within NCCN favorable-risk acute myeloid leukemia. Leuk Res. 2018;65:67–73.
29. Estey EH. Acute myeloid leukemia: 2019 update on risk-stratification and management. Am J Hematol. 2018;93(10):1267–91.
30. Estey E. Acute myeloid leukemia: 2016 Update on risk-stratification and management. Am J Hematol. 2016;91(8):824–46.
31. Estey EH. Acute myeloid leukemia: 2014 update on risk-stratification and management. Am J Hematol. 2014;89(11):1063–81.
32. Powers RK, Goodspeed A, Pielke-Lombardo H, Tan AC, Costello JC. GSEA-InContext: identifying novel and common patterns in expression experiments. Bioinformatics. 2018;34(13):i555-i64.

33. Hackl H, Steinleitner K, Lind K, Hofer S, Tosic N, et al. A gene expression profile associated with relapse of cytogenetically normal acute myeloid leukemia is enriched for leukemia stem cell genes. Leuk Lymphoma. 2015;56(4):1126–8.
34. Staber PB, Linkesch W, Zauner D, Beham-Schmid C, Guelly C, Schauer S, et al. Common alterations in gene expression and increased proliferation in recurrent acute myeloid leukemia. Oncogene. 2004;23(4):894–904.
35. Dolnik A, Engelmann JC, Scharfenberger-Schmeer M, Mauch J, Kelkenberg-Schade S, Haldemann B, et al. Commonly altered genomic regions in acute myeloid leukemia are enriched for somatic mutations involved in chromatin remodeling and splicing. Blood. 2012;120(18):e83–92.
36. Moreno-Sanchez R, Rodriguez-Enriquez S, Marin-Hernandez A, Saavedra E. Energy metabolism in tumor cells. FEBS J. 2007;274(6):1393–418.
37. Ganapathy-Kanniappan S. Molecular intricacies of aerobic glycolysis in cancer: current insights into the classic metabolic phenotype. Crit Rev Biochem Mol Biol. 2018;53(6):667–82.
38. Lu J, Bottcher M, Walther T, Mougiakakos D, Zenz T, Huber W. Energy metabolism is co-determined by genetic variants in chronic lymphocytic leukemia and influences drug sensitivity. Haematologica. 2019;104(9):1830–40.
39. Wilson RB, Solass W, Archid R, Weinreich FJ, Konigsrainer A, Reymond MA. Resistance to anoikis in transcoelomic shedding: the role of glycolytic enzymes. Pleura Peritoneum. 2019;4(1):20190003.
40. Li X, Qian X, Jiang H, Xia Y, Zheng Y, Li J, et al. Nuclear PGK1 Alleviates ADP-Dependent Inhibition of CDC7 to Promote DNA Replication. Mol Cell. 2018;72(4):650–60. e8.

Tables

Table 1 The names, abbreviations, functions and EPC scores for the 32 hub genes

EPC rank	EPC score	Gene Symbol	Full name of genes and functions of protein encoded by corresponding gene
1	13.198	PGK1	Phosphoglycerate Kinase 1, a glycolytic enzyme, also a cofactor for polymerase alpha, and is
			also secreted by tumor cells where it participates in distinct functions
2	13.02	PFKL	Phosphofructokinase, a glycolytic enzyme catalyzes the phosphorylation of D-fructose
			6-phosphate (the first committing step of glycolysis)
3	12.913	GPI	Glucose-6-Phosphate Isomerase, a glucose phosphate isomerase, also has a moonlighting
			protein based on its ability to perform mechanistically distinct functions.
4	12.874	ALDOC	Aldolase, Fructose-Bisphosphate C, a glycolytic enzyme encodes a member of the class I
			fructose-biphosphate aldolase gene family
5	12.863	TPI1	Triosephosphate Isomerase 1, two identical proteins invovled in glycolysis and gluconeogenesis
6	12.859	PFKP	Phosphofructokinase, a platelet-specific isoform of phosphofructokinase involved in glycolysis
			regulation, also plays a role in metabolic reprogramming in some cancers
7	12.845	HK2	Hexokinase 2, phosphorylates glucose to produce glucose-6-phosphate, the first step in most
			glucose metabolism pathways
8	12.834	ALDOA	Aldolase, Fructose-Bisphosphate A, a glycolytic enzyme encodes a member of the class I
			fructose-bisphosphate aldolase protein family
9	12.832	PFKM	Phosphofructokinase, a tetramer phosphofructokinase, which catalyzes the phosphorylation of
			fructose-6-phosphate to fructose-1,6-bisphosphate
10	12.794	H6PD	Hexose-6-Phosphate Dehydrogenase, p articipates in carbohydrate binding and glucose-6-
			phosphate dehydrogenase activity
11	12.792	CDKN1C	Cyclin Dependent Kinase Inhibitor 1C, a tight-binding, strong inhibitor of several G1 cyclin/Cdk

			complexes and a negative regulator of cell proliferation
12	12.782	HK1	Hexokinase 1, phosphorylates glucose to produce glucose-6-phosphate, the first step in most
			glucose metabolism pathways
13	12.748	ENO3	Enolase 3, plays a role in muscle development and regeneration
14	12.747	GAPDHS	Glyceraldehyde-3-Phosphate Dehydrogenase, Spermatogenic, plays an important role in
			carbohydrate metabolism
15	12.706	ALDOB	Aldolase, Fructose-Bisphosphate B, a tetrameric glycolytic enzyme related with glucose
			metabolism and citrate cycle (TCA cycle)
16	12.683	TALDO1	Transaldolase 1, a key enzyme of the nonoxidative pentose phosphate pathway
17	12.679	G6PD	Glucose-6-Phosphate Dehydrogenase, a cytosolic enzyme whose main function is to produce
			NADPH
18	12.673	PKLR	Pyruvate Kinase L/R, a pyruvate kinase that catalyzes the transphosphorylation of
			phohsphoenolpyruvate into pyruvate and ATP, which is the rate-limiting step of glycolysis
19	12.647	TKTL1	Transketolase Like 1, a transketolase that acts as a homodimer and links with the pentose
			phosphate pathway with the glycolytic pathway
20	12.595	PKM	Pyruvate Kinase M1/2, a pyruvate kinase involved in glycolysis
21	12.584	ENO1	Enolase 1, functions as a glycolytic enzyme and also function as a tumor suppressor
22	12.569	PGM1	Phosphoglucomutase 1, an isozyme of phosphoglucomutase (PGM) which catalyzes the transfer
			of phosphate between the 1 and 6 positions of glucose
23	12.551	TKT	Transketolase, a thiamine-dependent enzyme which plays a role in the channeling of excess
			sugar phosphates to glycolysis in the pentose phosphate pathway

Continued

EPC rank	EPC score	Gene Symbol	Full name of genes and functions of protein encoded by corresponding gene
24	12.546	PGAM2	Phosphoglycerate Mutase 2, a dimeric enzyme in the glycolytic pathway
25	12.335	LDHB	Lactate Dehydrogenase B, a lactate dehydrogenase enzyme which catalyzes the interconversion
			of pyruvate and lactate
26	12.307	PGAM1	Phosphoglycerate Mutase 1, a mutase that catalyzes the reversible reaction of
			3-phosphoglycerate (3-PGA) to 2-phosphoglycerate (2-PGA) in the glycolytic pathway
27	12.107	PGAM4	Phosphoglycerate Mutase Family Member 4, a mutase that catalyzes the reversible reaction of
			3-PGA to 2-PGA in the glycolytic pathway
28	12.038	FBP2	Fructose-Bisphosphatase 2, a gluconeogenesis regulatory enzyme that catalyzes the hydrolysis
			of fructose 1,6-bisphosphate to fructose 6-phosphate
29	11.918	FBP1	Fructose-Bisphosphatase 1, a gluconeogenesis regulatory enzyme that catalyzes the hydrolysis
			of fructose 1,6-bisphosphate to fructose 6-phosphate
30	11.611	ENO2	Enolase 2, participates in magnesium ion binding and phosphopyruvate hydratase activity
31	11.191	GCK	Glucokinase, a member of the hexokinase family phosphorylates glucose to produce glucose-6
			-phosphate, the first step in most glucose metabolism pathways
32	11.013	BPGM	Bisphosphoglycerate Mutase, a multifunctional enzyme that catalyzes 2,3-DPG synthesis and
			2,3-DPG degradation

Table 2 The clinical characteristics of the 50 patients with acute myeloid leukemia

Variables	PGK1 expression level		P-value
	Low-expression (n=25)	High-expression (n=25)	
Gender, female, n (%)	12 (48.0%)	8 (32.0%)	0.248
Age (months), median (range)	83 (9-166)	67 (8-145)	0.347
WBC count (*10^9/L), median (range)	23.61 (1.50-226.00)	15.50 (1.80-275.90)	0.907
Hgb level (*g/L), median (range)	87 (29-111)	85 (38-122)	0.554
PLT count (*10^9/L), median (range)	62 (19-217)	43 (11-229)	0.187
Gene rearrangements, n(%)	25	25	0.83
AML1/ETO	8 (32.0%)	8(32.0%)	-
MLLr	4 (16.0%)	2 (8.0%)	-
CBF/MYH11	4 (16.0%)	4 (16.0%)	-
Others or Negative	9 (36.0%)	11 (44.0%)	-
Gene mutations, n(%)	25	25	0.109
c-KIT	2 (8.0%)	6 (24.0%)	-
CEBPα double mutation	1 (4.0%)	1 (4.0%)	-
FLT3-ITD	2 (8.0%)	0 (0%)	-
NPM1	2 (8.0%)	0 (0%)	-
PTPN11	1 (4.0%)	0 (0%)	-
Others or Negative	17 (68.0%)	18 (72.0%)	-
Cytogenetics, n(%)	25	25	0.339
Favorable	15 (60.0%)	10 (40.0%)	-
Intermediate	6 (24.0%)	6 (24.0%)	-
Adverse	3 (12.0%)	8 (32.0%)	-
Undetectable	1 (4.0%)	1 (4.0%)	-
FAB subtype	25	25	0.375
AML-M2	12 (48.0%)	11 (44.0%)	-
AML-M4	6 (24.0%)	4 (16.0%)	-

AML-M5	4 (16.0%)	8 (32.0%)	-
AML-M7	0 (0%)	1 (4.0%)	-
AML-unclassified	3 (12.0%)	1 (4.0%)	-
AML risk group	25	25	0.019
Low risk	16(64.0)	7(28.0)	-
Intermediate risk	6(24.0)	8(32.0)	-
High risk	3(12.0)	10(40.0)	-
First induction, CR, n(%)	22 (88.0%)	14 (56.0%)	0.027
Second induction, CR, n(%)	24 (96.0%)	18 (72.0%)	0.054
HSCT, n(%)	6 (24.0%)	11 (44.0%)	0.136
Relapse, n(%)	1 (4.0%)	7 (28.0%)	0.747
Deaths, n(%)	3 (12.0%)	11 (44.0%)	0.027
5-year CIR	4.3±4.3%	47.0±13.2%	0.001
5-year EFS	88.0±6.5%	31.1±9.4%	<0.001
5-year OS	88.0±6.5%	56.0±9.9%	0.007

AML: acute myeloid leukemia; PGK1: phosphoglycerate kinase 1; WBC: white blood cell; Hgb: hemoglobin; PLT: platelet; FAB: French-American-British; CR: complete remission; HSCT: hematopoietic stem cell transplantation; CIR: cumulative incidence of relapse; EFS: event-free survival; OS: overall survival.

Table 3 IC50 of DNR and Ara-C of U937 and K562 cell lines

Drugs	Cell lines	IC50 (95%CI) μmol/L		Folds	P-value
		shNC	shPGK1		
DNR	U937	13.36 (10.930-16.566)	1.865 (1.423-2.345)	7.16	<0.001
	K562	11.654 (8.808-15.759)	4.791 (3.622-6.231)	2.43	0.005
Ara-C	U937	19.577 (15.903-24.686)	4.047 (3.355-4.829)	4.84	<0.001
	K562	18.596 (15.097-23.446)	3.519 (2.723-4.430)	5.28	<0.001

IC50: half maximal inhibitory concentrations; DNR: daunorubicin; Ara-C: cytarabine; CI: confidence interval

Figures

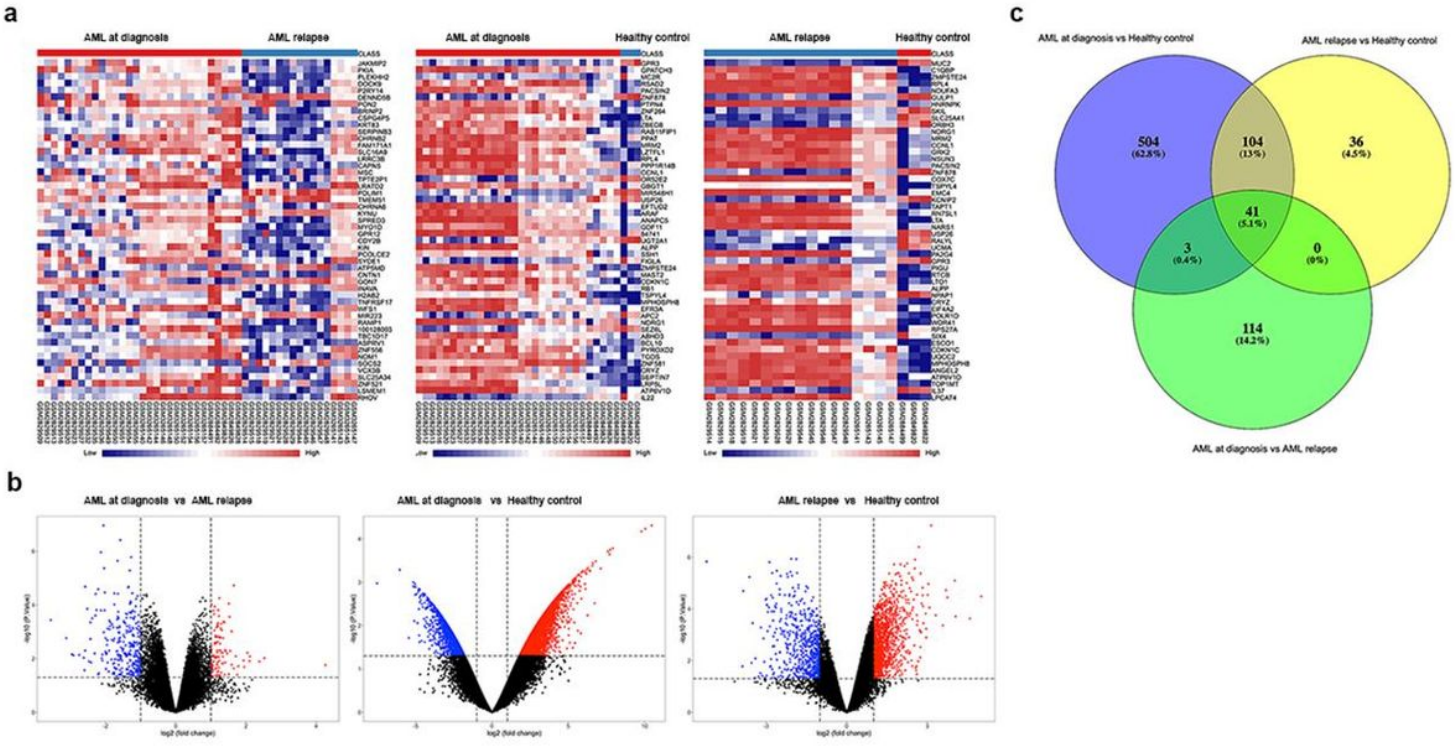

Figure 1

Figure 1

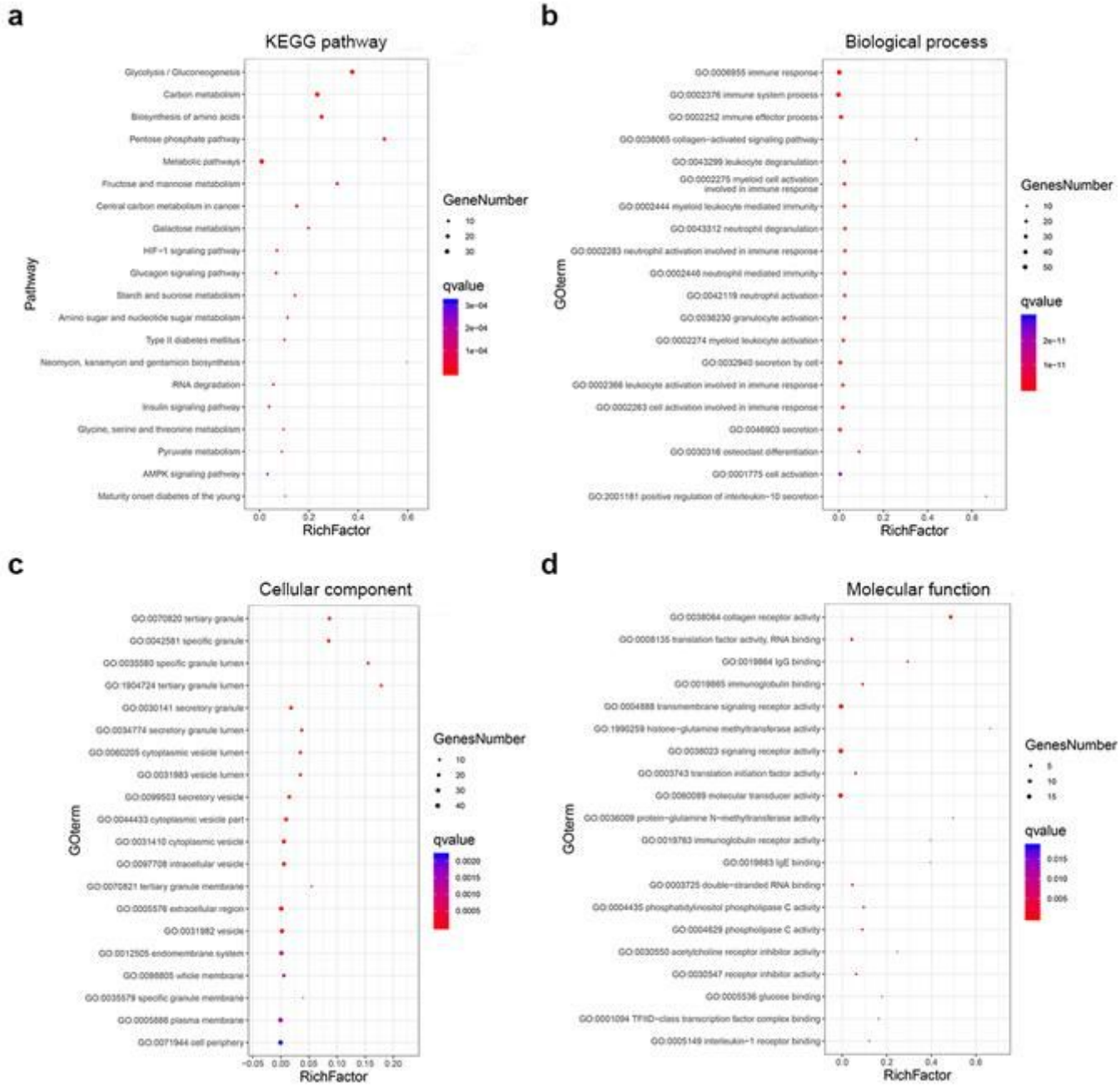

Figure 2

Figure 2

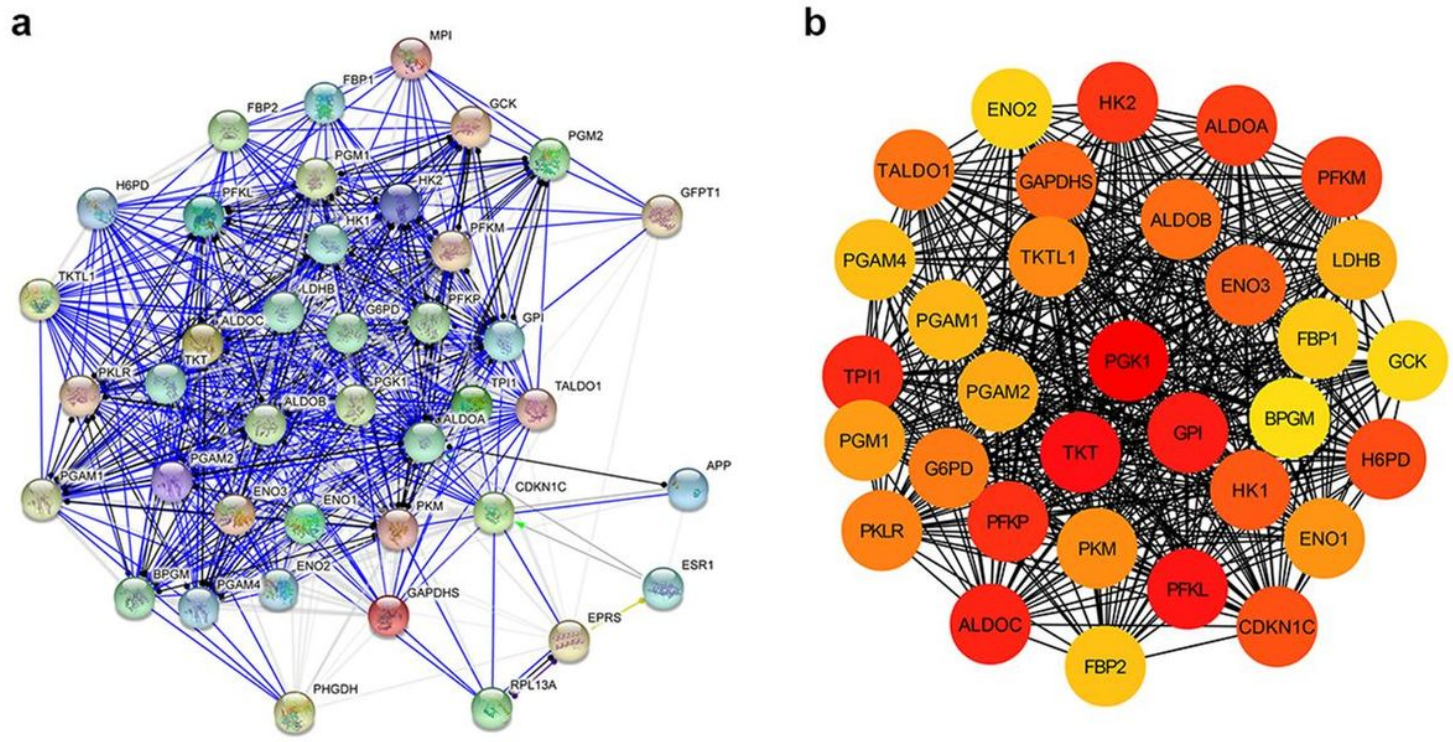

Figure 3

Figure 3

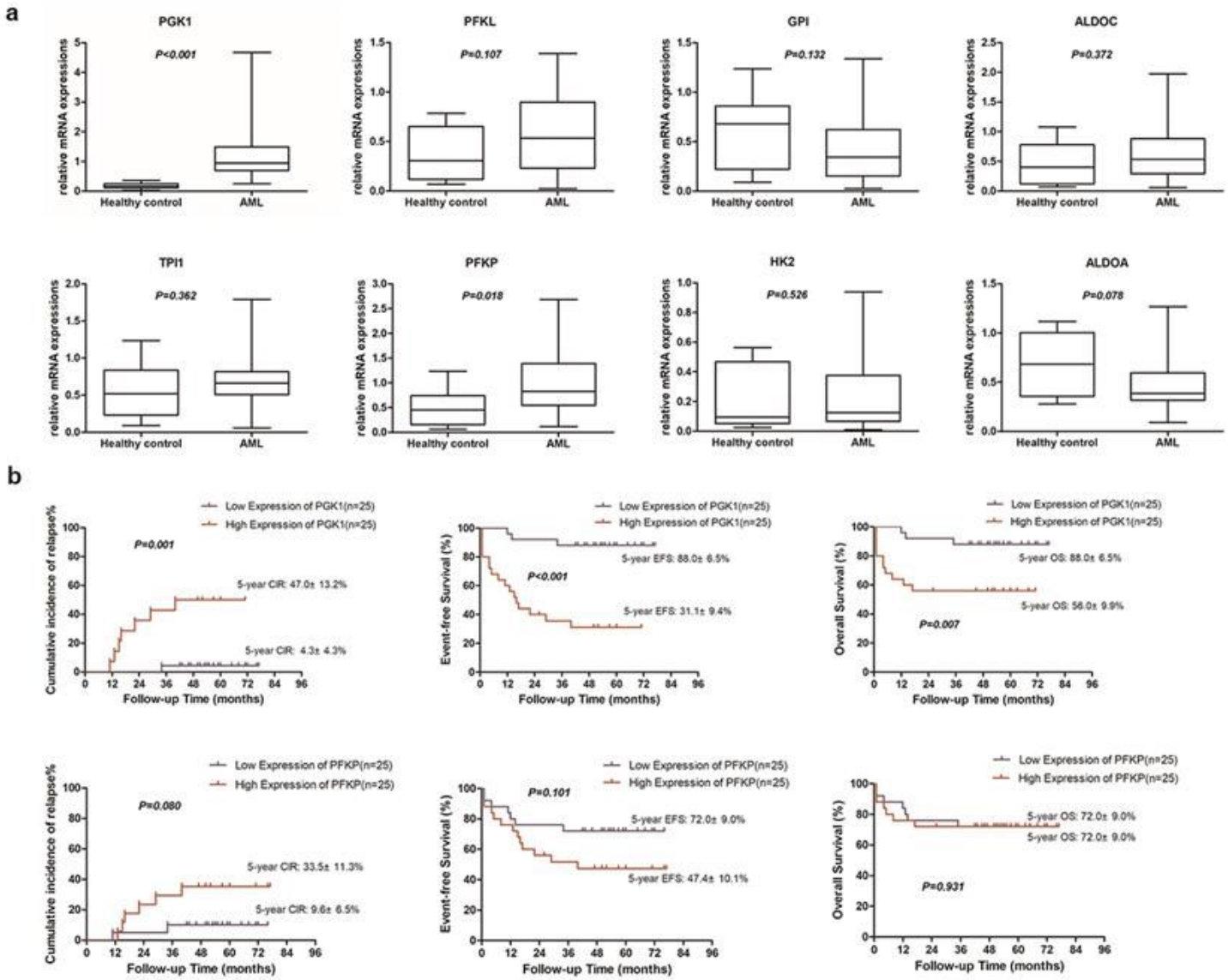

Figure 4

Figure 4

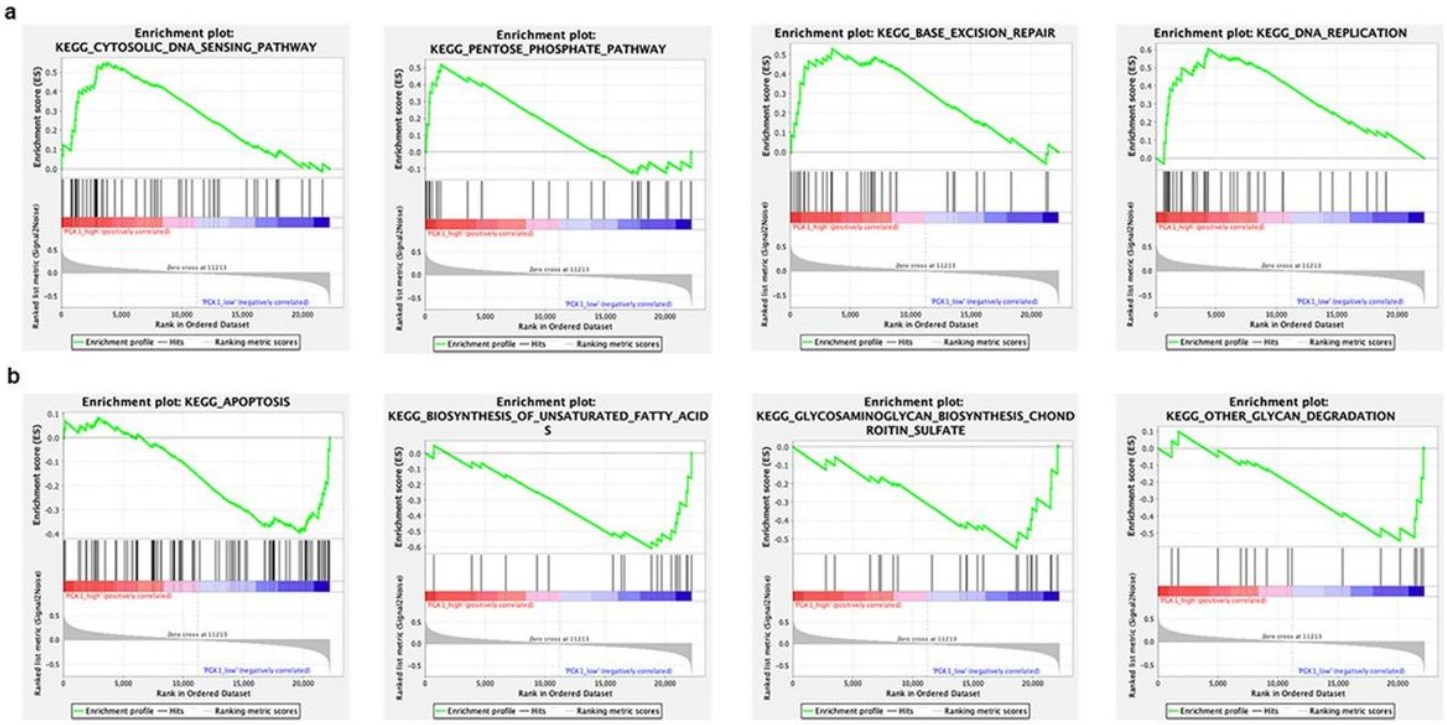

Figure 5

Figure 5

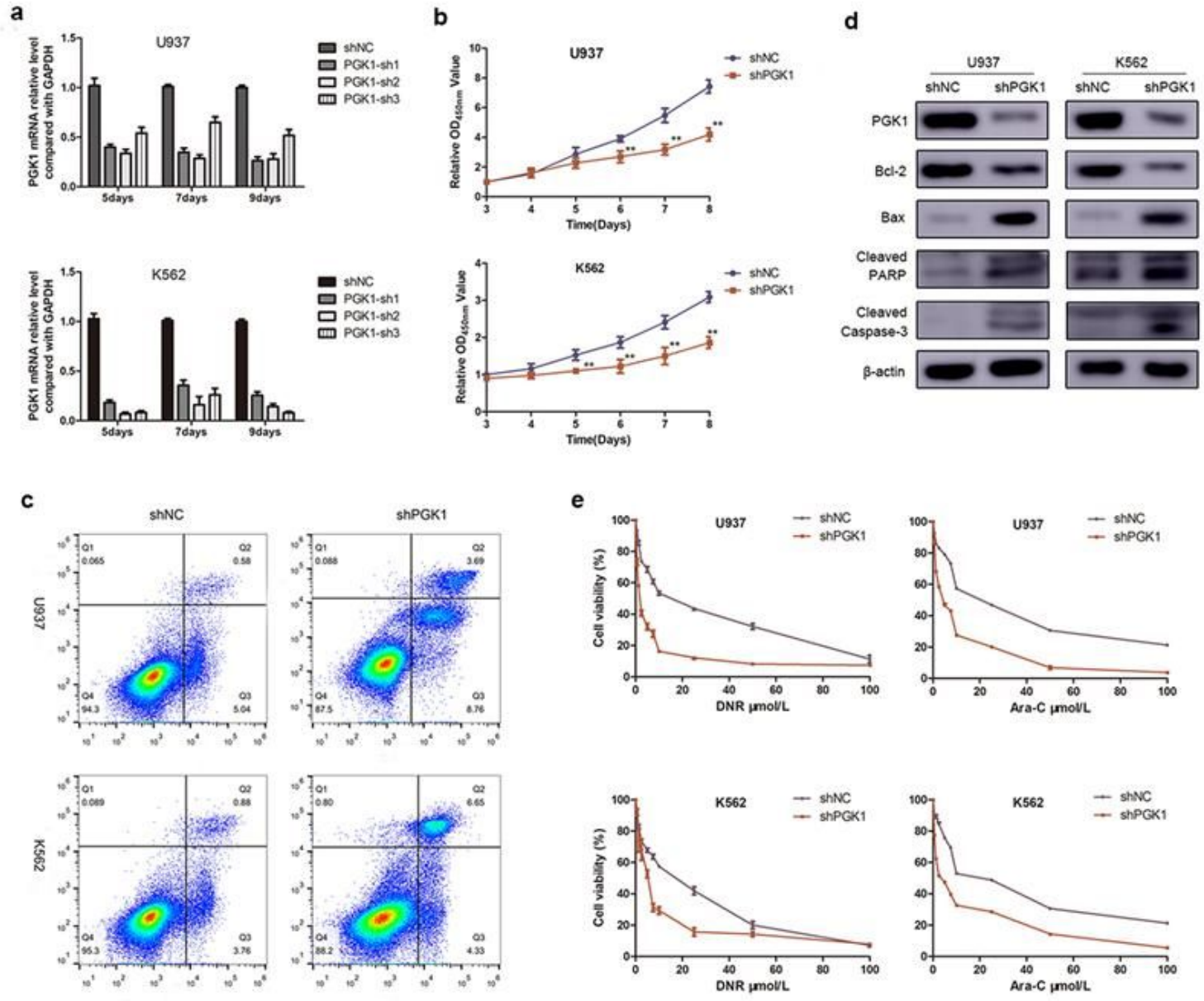

Figure 6

Figure 6

Supplementary Files

This is a list of supplementary files associated with this preprint. Click to download.

- SupplementaryFigure2.tif
- SupplementaryTable2.doc
- SupplementaryTable1.doc
- SupplementaryFigure1.tif